29. MINERALOGY AND INCIPIENT DIAGENESIS OF PIGMY BASIN SEDIMENTS, HOLE 619, DEEP SEA DRILLING PROJECT LEG 96[1]

Thomas T. Tieh, Steven V. Stearns, and Bobby J. Presley, Texas A&M University[2]

ABSTRACT

Pigmy Basin sediments cored in Hole 619 of Deep Sea Drilling Project Leg 96 are silty clays composed, on the average, of <1% sand, 37% silt, 48% clay, and 14% carbonate minerals. Except for minor grain dissolution in some silt grains, there is no distinctive variation with depth in either composition or texture of the sand- and silt-sized minerals. This suggests a constant source of sediment supply and little diagenetic alteration of these size fractions.

Clay minerals are dominated by smectite or, more precisely, montmorillonite. On the average, the clay-sized fraction consists of 48% smectite and mixed layer minerals, 30% illite, and 23% total kaolinite and chlorite. There appears to be a slight decrease in smectite and concomitant increases in other clay minerals with depth. These changes are further substantiated by the variations of ammonium acetate exchangeable K^+, Mg^{2+}, and Na^+ in bulk samples. Thus, incipient diagenesis of Pigmy Basin sediments is evidenced in the mineralogical and associated chemical characteristics of the clay fractions.

INTRODUCTION

The objectives of this mineralogical study of Pigmy Basin sediments were (1) to determine mineralogical variations through time in this sequence of largely pelagic to hemipelagic sediments and (2) to detect any subtle changes in mineralogy or related chemical characteristics in the sediments, particularly in the clay fractions, that may have arisen from incipient diagenesis.

The Pigmy Basin is an intraslope basin of the blocked-canyon type (Bouma, 1983). Hole 619 was drilled in a water depth of 2273 m and reached a total penetration of 208.7 m. Sediments cored consist predominantly of dark grey pelagic to hemipelagic clays, with occasional thin layers of sandy and silty materials. The latter become more common with depth, especially below 150 m, and are thought to be fine-grained turbidites (see Site 619 chapter, this volume).

SAMPLES AND METHODS

A total of 16 samples, from the depth interval of 6 to 150 m below seafloor, were examined. All samples selected were clay rich in appearance; sandy or silty layers were avoided. Below 150 m, the sediments are typically coarser grained. Except for the two deepest samples (Samples 619-17-2, 58–60 cm at 147.8 m and 619-17-3, 58–60 cm at 149.3 m), which were obtained from a chaotic mud clast deposit, all samples are of a pelagic–hemipelagic nature.

Laboratory analysis of each sample consisted of the following: (1) size fractionation into sand (>63 μm), silt (63–2.0 μm), and clay (<2.0 μm) fractions; (2) optical microscopy study of the sand fraction; (3) study of the silt fraction by combined scanning electron microscopy (SEM), x-ray diffraction (XRD), and optical microscopy methods; (4) study of the clay fraction by XRD after cation saturation and heating, and chemical methods that include cation exchange capacity (CEC) and total K determinations; (5) detailed study of one sample (Sample 619-6-3, 125–129 cm; 43.8 m sub-bottom depth) which involved separation of the clay fraction into coarse (2.0–0.2 μm) and fine (<0.2 μm) fractions, and analysis of both fractions by infrared spectroscopy and transmission electron microscopy in addition to the above methods; and (6) SEM surveys of untreated bulk samples as well as determination of cations exchangeable by ammonium acetate.

Grain Size Distribution, Carbonate and Iron Content

Sample treatments before size fractionation included the following: (1) removal of carbonates, which occur largely as cementing agents, but also in the form of biogenic or detrital grains; (2) removal of organic matter and Mn oxide; and (3) removal of free iron. Freeze-dried samples were first dispersed in a pH 5 sodium acetate and acetic acid solution, at a constant fluid to sediment ratio, and heated to near boiling. Supernatant fluids were removed and analyzed for Ca and Mg content by atomic absorption (AA). Estimates of total carbonate content (Table 1) were computed by assuming all dissolved Ca and Mg were originally in carbonate form. Following this, organic matter and Mn oxides were removed by washing and heating the samples in H_2O_2. No attempt was made to determine the exact amount of organic matter or Mn oxide. Finally, the free iron was removed from the samples using the standard sodium dithionite leach of Mehra and Jackson

Table 1. Grain size distribution, carbonates, and Fe_2O_3 content of samples from Hole 619.[a]

Core-Section (interval in cm)	Sub-bottom depth (m)	Sand	Silt	Clay	Carbonates	Fe_2O_3
1-4, 50–52	6.00	0.0	34.0	54.6	11.0	0.39
3-4, 125–127	16.25	0.0	34.0	50.4	12.3	0.31
4-3, 125–127	24.45	0.0	36.6	50.6	12.4	0.38
5-1, 125–127	31.15	2.5	38.5	45.9	12.7	0.37
5-5, 50–52	36.40	0.0	39.0	52.0	8.5	0.48
6-3, 125–129	43.85	49.0[b]		50.0	11.0	0.47
6-5, 125–129	46.85	0.5	50.2	35.7	13.2	0.36
7-3, 125–127	53.55	0.5	40.3	30.3	14.2	0.52
8-2, 125–127	61.75	0.5	41.1	42.7	15.2	0.54
9-2, 13–14	70.33	0.0	37.8	43.8	17.8	0.57
10-3, 94–95	82.34	0.5	36.5	55.8	18.3	0.49
12-1, 42–43	98.02	0.0	34.0	49.8	15.6	0.56
13-2, 42–43	109.12	2.5	31.0	49.5	16.4	0.59
15-1, 42–45	136.42	0.5	34.8	49.1	15.0	0.62
17-2, 58–60	147.78	3.4	30.0	50.8	15.3	0.55
17-3, 58–60	149.28	0.5	33.5	56.3	9.2	0.46

[a] All values are in weight percent.
[b] Value given is sand + silt percentage (sand and silt were not separated in this sample).

[1] Bouma, A. H., Coleman, J. M., Meyer, A. W., et al., *Init. Repts. DSDP*, 96: Washington (U.S. Govt. Printing Office).

[2] Addresses: (Tieh, Stearns) Department of Geology, Texas A&M University, College Station, TX 77843; (Presley) Department of Oceanography, Texas A&M University, College Station, TX 77843.

(1960). The amounts of free iron were determined from the supernatant solutions by atomic absorption, and expressed as percent Fe_2O_3 (Table 1).

After these treatments, the samples were size fractionated by wet sieving and centrifugation methods. Table 1 summarizes the size distribution, percentage carbonate, and percentage free Fe_2O_3 of the samples studied.

Sand and Silt Analysis

Oil-immersion mounts of the sand and silt fractions were studied under a petrographic microscope. The silt fractions were further examined with SEM, and at least one representative field of view from each sample was recorded photographically. Because of the difficulties of quantitative analysis of silt with optical microscopy or SEM methods, split portions of each silt fraction were finely ground to <2.0 μm in acetone, pressed into a powder mount, and analyzed by XRD.

Clay Analysis

Initially, the clay fraction from one sample (619-6-3, 125–129 cm at 43.8 m depth) was chosen, for standardization purposes, to be analyzed in as much detail as possible. A portion of the clay fraction from this sample was analyzed for CEC and total K, and by XRD; a second portion was further fractionated into coarse (2.0–0.2 μm) and fine (<0.2 μm) clays. Each of these fractions was studied in the following manner:

1. XRD that includes saturation with Mg^{2+} and glycolation, K^+ saturation, heating of the K^+-saturated sample to 300°C, and to 500°C,
2. infrared spectroscopic analysis and,
3. transmission electron microscopy analysis of the fine clay fraction.

Cation exchange capacity (CEC) was determined for the clay fraction of Sample 619-6-3, 125–129 cm by first saturating the sample with Ca^{2+} and weighing it to determine the total amount of interstitial and adsorbed Ca^{2+}. A Mg^{2+} solution was then used to replace the Ca^{2+} on the exchange sites as well as any interstitial Ca^{2+}. The total amount of Ca^{2+} removed in the Mg^{2+} solution washes was then determined using atomic adsorption. Subsequently, exchange capacity of K^+ by NH_4^+ was determined in a similar way using the same samples. All CEC determinations were run with duplicates. Results of the Ca^{2+}/Mg^{2+} and K^+/NH_4^+ CEC determinations were used to estimate the total amount of smectite and vermiculite.

Quantitative determination of illite was obtained by first fully digesting the sample in HF, and then analyzing for total K. The assumption made during the calculations was that 1% K_2O represents 10% illite and mica in the sample (Alexiades and Jackson, 1966), which is subject to error arising from the presence of K feldspars. The amount of total kaolinite and chlorite was determined by subtracting from 100 the amount of expandable clays (smectite and vermiculite) and that of illite.

Clay fractions separated from all the other samples were analyzed by XRD in the same manner (i.e., cation saturation and heating) as for Sample 619-6-3, 125–129 cm. Several selected samples, which show a range in diffraction peak heights of the various clay minerals, were also analyzed for CEC and total K. The purpose of these analyses was to determine the relationship between chemical data (CEC and total K) and diffraction peak heights, so that quantitative clay analysis could be made on all the other samples strictly on the basis of relative heights of diffraction peaks. Quartz and feldspars in the clay fractions were not included in quantification of clays because they do not show recognizable differences in diffraction peak heights in the samples studied.

Using diffraction peak height (PH) or peak area as a means of quantifying the abundance of the different clay minerals in a sample is a common practice when dealing with mudstones or shales (Biscaye, 1965; Schultz, 1964; Devine et al., 1972). In this study it was found that there is a close relationship between the CEC and the height of the 18-Å peak (smectite) of the Mg-glycolated XRD pattern. Further, total K is also proportional to the 10-Å (illite) peak height. Empirically, from the Mg-glycolated pattern, relative abundances of the smectite and illite are

$$\text{smectite (\%)} = \frac{1.5 \times \text{PH of 18 Å}}{\text{PH of (18 Å + 7 Å)} + (1.5 \times \text{PH of 10 Å})}$$

$$\text{illite (\%)} = \frac{1.5 \times \text{PH of 10 Å}}{\text{PH of (18 Å + 7 Å)} + (1.5 \times \text{PH of 10 Å})}$$

The abundance of total kaolinite and chlorite is then 100 − [smectite (%) + illite (%)] (Table 2).

Exchangeable Cation Analysis

Ammonium exchangeable cations were determined for each of the samples by first suspending 4 g of freeze-dried, untreated, and unfractionated sediment in distilled water to remove interstitial cations (soluble salts). After this initial wash, samples were rinsed three times with a total of 100 ml of pH 7 1 *N* ammonium acetate (NH_4OAc) solution. Supernatant fluids from these washes were then analyzed using AA to determine concentrations of Na^+, K^+, Ca^{2+}, Mg^{2+}, Sr^{2+}, and Fe^{2+}.

RESULTS

Texture and Mineralogy of Sand Fractions

Of the 16 samples analyzed, sand constitutes between 2.5 and 3.4% in three samples, 0.05% in six, and is not detected in any of the others (Table 1). Examination of the sand fractions by the oil-immersion method under a petrographic microscope shows that the sand grains are predominantly subrounded; very angular and very well-rounded grains are only occasionally present. No distinctive differences in grain morphology are recognizable between the samples. In the three samples where 2.5% or more sand is present, spaced over a depth range of more than 100 m (31.15 to 147.78 m; Table 1), point counting yields an average of 81% quartz, 8% feldspar, 10% rock fragments, and traces of other constituents that include micas, hornblende, apatite, garnet, epidote, and opaques.

Portions of the sand fractions were observed with the SEM to determine if partial grain dissolution or authigenic overgrowth or outgrowth, indicative of diagenesis, is present. Such alterations were not apparent. Further, surface textures of sand grains show no observable trends with depth. Dissolution of sand grains in Quaternary

Table 2. Clay mineral composition of Hole 619 samples.[a]

Core-Section (interval in cm)	Sub-bottom depth (m)	Smectite + mixed layer (%)	Kaolinite + chlorite (%)	Illite + mica (%)
1-4, 50–52	6.00	66	15	19
		(48)	(20)	(32)
3-4, 125–127	16.25	65	15	20
4-3, 125–127	24.45	58	15	27
5-1, 125–127	31.15	47	22	30
5-5, 50–52	36.40	63	19	25
6-3, 125–129	43.85	30	29	41
		(30)	(24)	(46)
6-5, 125–129	46.85	46	21	32
7-3, 125–127	53.55	48	22	30
8-2, 125–127	61.75	38	25	37
9-2, 13–14	70.33	50	21	29
10-3, 94–95	82.34	24	34	42
		(28)	(28)	(44)
12-1, 42–43	98.02	43	24	33
13-2, 42–43	109.12	42	28	30
15-1, 42–45	136.42	49	22	29
17-2, 58–60	147.78	53	25	23
17-3, 58–60	149.28	49	26	25
		(39)	(28)	(33)

[a] Values in parentheses were derived using CEC and total K data.

sediments is most frequently displayed by ferromagnesian silicate minerals (Hutton, 1959), but such minerals are scarce in these samples.

Texture and Mineralogy of Silt Fractions

Silt constitutes from 30 to 50% of the 16 samples studied, with an average of 37% (Table 1). Optical microscopy examination of the silt fractions reveals the dominance of quartz and feldspars; occasional shard-like fragments are present, as well as traces of hornblende, zircon, and anatase. Figure 1A shows the variable nature of the texture and morphology of the silt in these samples. Features suggestive of grain dissolution and/or overgrowth were seen in numerous silt grains (Fig. 1B). Although some of these may have formed during sample preparation, it is believed that postdepositional silt-grain alteration has occurred because similar textures were also observed in untreated bulk samples. However, the overall amount of silt alteration, and the proportions of which is predepositional versus postdepositional, cannot be assessed. A search for volcanic glass shards, which are characterized by their shape and the usual presence of vesicles, proved to be unsuccessful. Shardlike grains occasionally seen under the petrographic microscope are thought to be highly angular fragments of quartz. The two ash beds identified at 41 m (see Site 619 chapter, this volume) were not sampled for this study.

X-ray diffractograms show only reflections characteristic of quartz and feldspars. Furthermore, all diffractograms of the silt fractions are virtually identical in peak position and relative peak height. This indicates that the composition of the silt fraction does not vary greatly with depth. Trace minerals identified under the petrographic microscope were not detected on the diffractograms because of their scarcity.

Clays in the Pigmy Basin Sediments

For the samples where both chemical and XRD data are available, the relationship between the CEC-determined and the XRD-peak-height–determined smectite abundance is shown in Figure 2, and that between total K and peak-height determined illite abundances is shown in Figure 3. These figures provide an indication of the accuracy of the results reported in Table 2. Scattering in Figure 3 is at least partially caused by the presence of other K-bearing minerals, particularly the feldspars.

Table 2 shows that clay minerals exhibit a general decrease with depth in the abundance of smectite and mixed-layer clays and, correspondingly, a general increase in kaolinite–chlorite and illite. These trends are not sys-

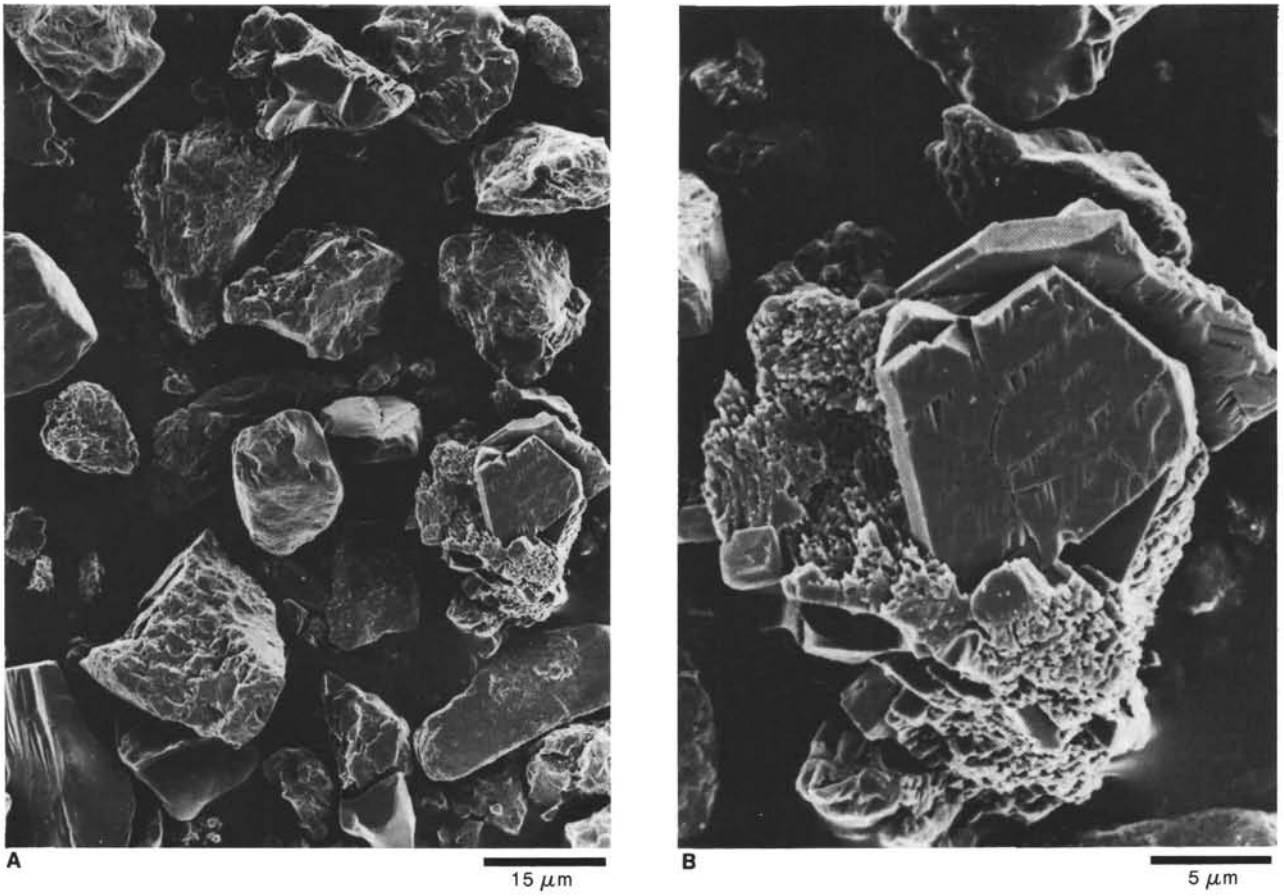

Figure 1. Scanning electron micrographs of typical silt grains in Pigmy Basin Sample 619-10-3, 94–95 cm. Figure 1A shows the generally variable nature, from angular to rounded, of the silt grains; Figure 1B is a close-up view of a feldspar grain visible on the right side of Figure 1A, showing pitting from incipient grain dissolution. The subhedral grain outline appears to be from overgrowth.

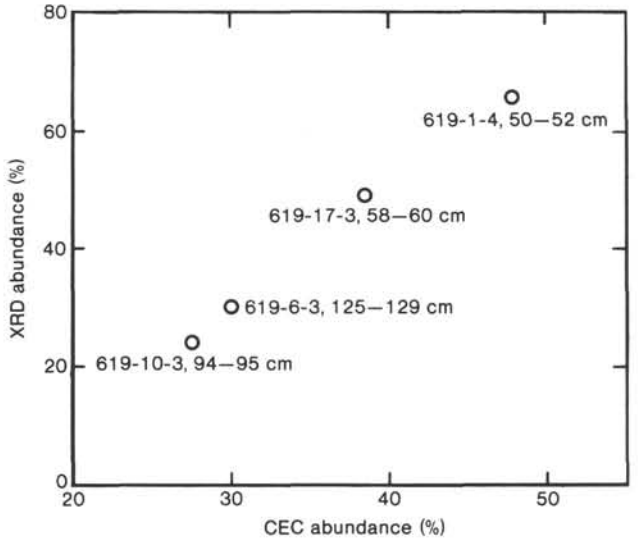

Figure 2. Relationship between abundance of smectite and mixed-layer minerals determined by cation exchange capacity (CEC) and that determined from selected x-ray diffraction (XRD) peak heights for four samples from Hole 619 (data given in Table 2).

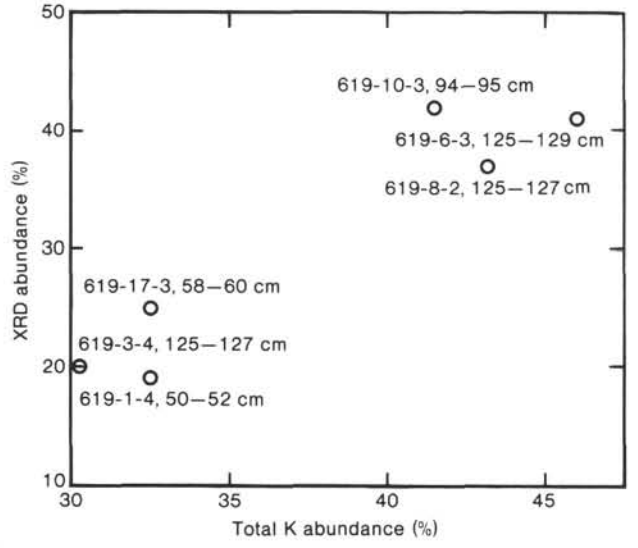

Figure 3. Relationship between abundance of illite + mica determined by total K analysis and that determined from selected x-ray diffraction (XRD) peak heights for six samples from Hole 619.

tematic and one particularly noticeable exception to these trends occurs in Sample 619-10-3, 94–95 cm. It is interesting to note that this sample also has the highest content of carbonates (see Table 1).

Clay Mineralogy of Sample 619-6-3, 125–129 cm

X-ray diffractograms of the coarse and fine clay fractions of Sample 619-6-3, 125–129 cm (at 43.8 m subbottom) are shown in Figures 4 and 5, respectively. In the coarse clay fraction, smectite, kaolinite, chlorite, illite, quartz, and possibly vermiculite are present (Fig. 4). The 18.3-Å peak in the Mg-glycolated sample clearly identifies smectite. With K^+ saturation and heating, the low-angle smectite peaks lose intensity while the 10-Å peak is strengthened. The 7.2-Å peak present in all treatments indicates the presence of kaolinite. In the K^+–550°C treatment, the 7.2-Å peak is greatly diminished because of the collapse of the kaolinite structure. The 3.55- and 3.59-Å doublet seen in the Mg^{2+} saturated sample is clear indication of the presence of both kaolinite and chlorite. A 14.2-Å chlorite peak is present in all treatments, but appears to collapse slightly to 13.8 Å at K^+–550°C, probably as a result of poorly developed interlayers. Strong 10.1- and 5.0-Å reflections, characteristic of illite, are seen in all treatments. The 3.33-Å peak, also characteristic of illite, is obscured by a strong 3.34-Å quartz peak. Quartz is also indicated by a peak at 4.26 Å. Vermiculite may also be present in the coarse clay fraction, but would be obscured by chlorite and smectite reflections.

As expected, the minerals identified in the fine clay fraction are more limited in number (Fig. 5). The diffractograms of this fraction are dominated by the major smectite peaks, which shift from 18.0 Å in the Mg glycolated sample to 10.1 Å after K^+ saturation and heating to 550°C. The kaolinite 7.1- and 3.56-Å peaks are also visible, as are the 10-, 5-, and 3.33-Å illite peaks. The strong 5-Å peak identifies the illite as a dioctahedral variety.

In general, the reflections in the fine-fraction diffractograms are noticeably broader than those in the coarse clay fraction, because of the smaller mean particle size. In addition, asymmetric peaks in the <0.2 μm diffractograms point out the abundance of very thin crystallites. A clear separation of the two clay fractions is shown by the lack of quartz and chlorite in the finer fraction.

Results of infrared (IR) spectroscopic analysis of the clay fractions are shown in Figure 6. Besides confirming the XRD results, the most important piece of information provided by the IR data is the identification of the smectite as a montmorillonite. In addition, broad peaks in the Si–O stretching region (1200–700 cm^{-1}) indicate that there is considerable substitution of Al for Si in the tetrahedral sheets of the montmorillonite. Peaks at 830 and 877 cm^{-1} in the fine clay fraction also show substitution of Fe and Mg for Al in the montmorillonite octahedral sheet. Well-defined 3690 cm^{-1} peaks in the OH stretching region (3750–3400 cm^{-1}) indicate kaolinite in both fractions. Chlorite identified in the coarse clay fraction appears to best match the patterns of Al-rich reference samples.

Clay minerals in Sample 619-6-3, 125–129 cm, consist of 30% expandable clays (dominantly smectite), 46% illite, and a total of 24% combined kaolinite and chlorite.

Transmission electron microscopic analysis of the fine clay fraction shows that it consists of plates of micaceous minerals (mica, illite, and/or chlorite) in a groundmass of structureless montmorillonite.

Exchangeable Cations in Bulk Sediment

The amounts of ammonium exchangeable cations in each bulk sediment sample, expressed in milliequivalents per 100 g, are presented in Table 3.

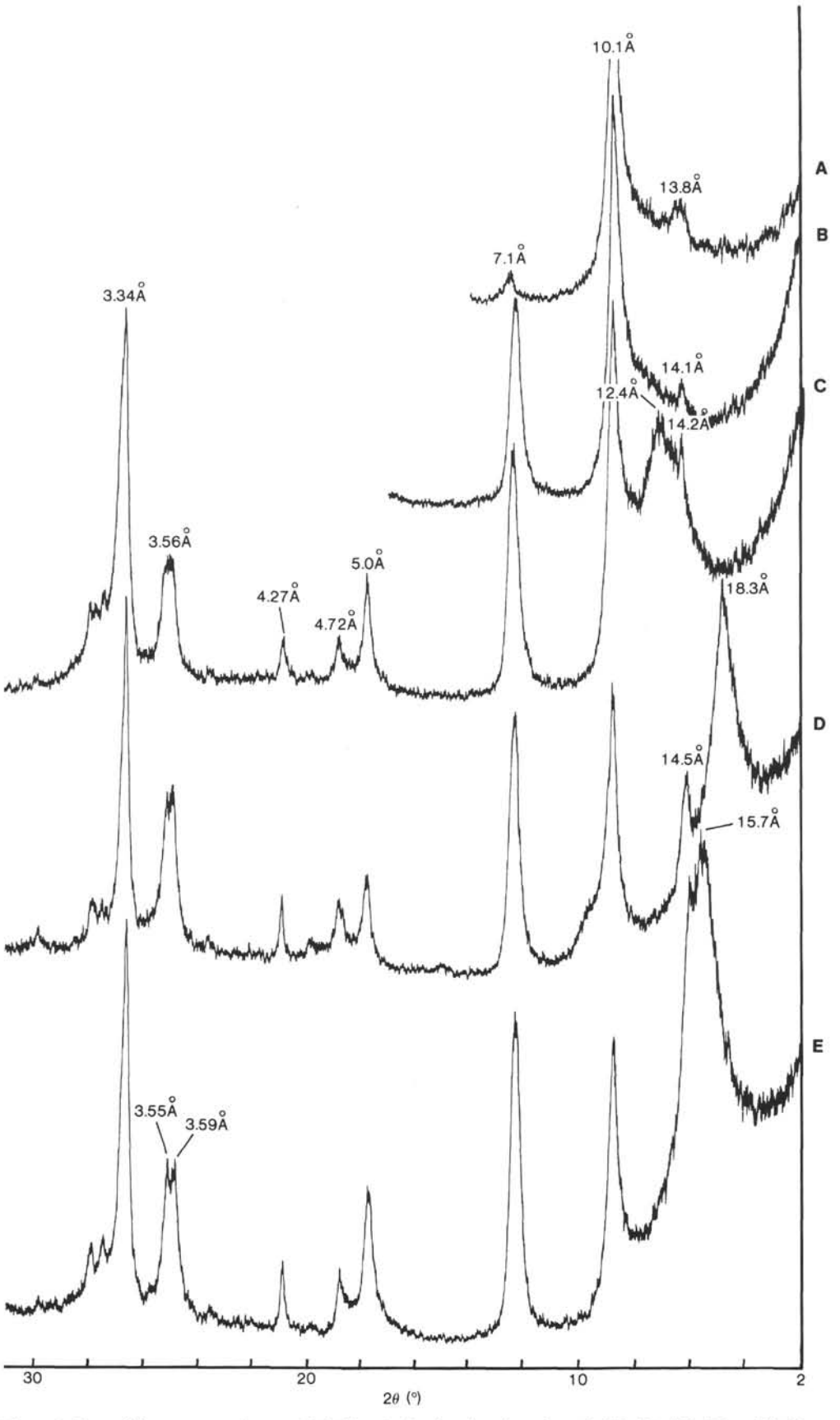

Figure 4. X-ray diffractograms of coarse (2.0–0.2 μm) clay fractions from Sample 619-6-3, 125–129 cm (43.85 m sub-bottom). A. K^+ saturated and heated to 550°C. B. K^+ saturated and heated to 300°C. C. K^+ saturated and unheated. D. Mg^{2+} saturated and glycolated. E. Mg^{2+} saturated.

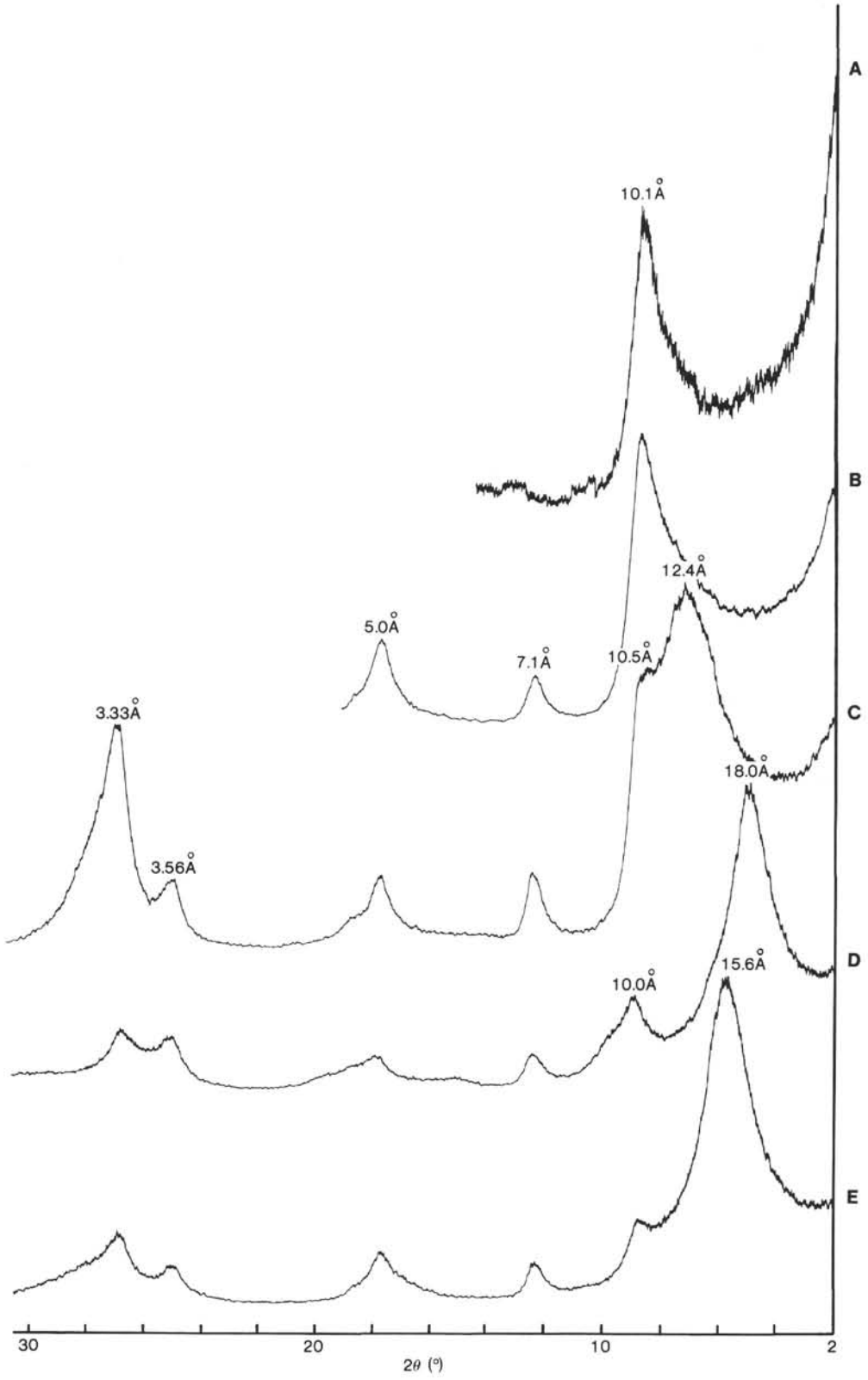

Figure 5. X-ray diffractograms of fine (<0.2 μm) clay fractions from Sample 619-6-3, 125–129 cm (43.85 m sub-bottom). A. K^+ saturated and heated to 550°C. B. K^+ saturated and heated to 300°C. C. K^+ saturated and unheated. D. Mg^{2+} saturated and glycolated. E. Mg^{2+} saturated.

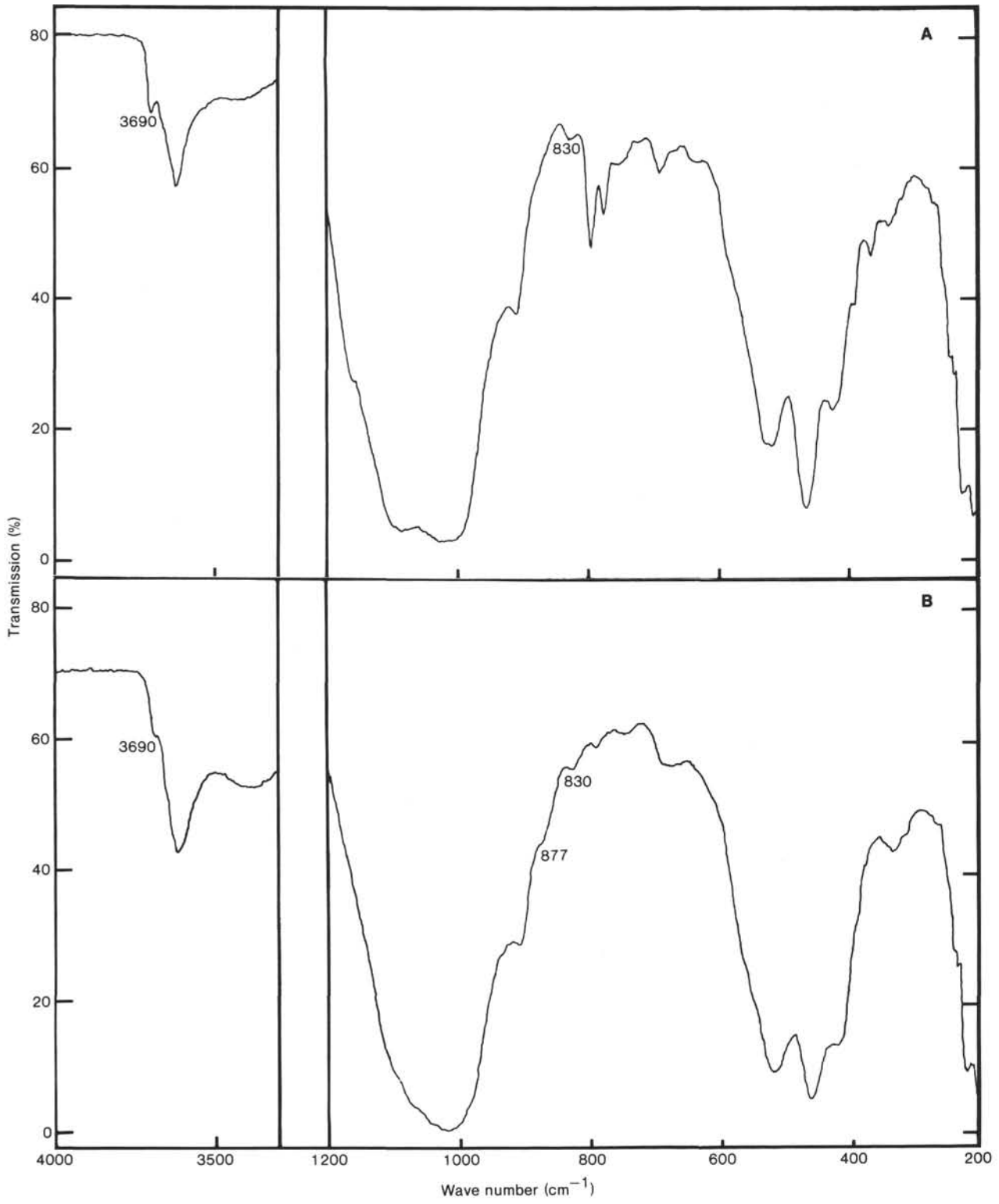

Figure 6. Infrared spectrographs of Sample 619-6-3, 125–129 cm. A. Coarse clay fraction (2.0–0.2 μm). B. Fine clay fraction (<0.2 μm).

SUMMARY AND DISCUSSION

All samples of Hole 619 in Pigmy Basin analyzed in this study consist of silty clay with the clay-sized material comprising approximately one half of each sample. Textural characteristics and mineralogical composition of the sand and the silt fractions do not show any recognizable systematic changes with depth, suggesting a constant source of supply during deposition of these sediments. Although diagenesis has caused partial dissolution of some silt grains, the exact extent or amount of dissolution cannot be assessed. Cementing materials,

Table 3. NH_4OAc exchangeable cations (in milliequivalents per 100 g) of samples from Hole 619.

Core-Section (interval in cm)	Sub-bottom depth (m)	Na^+	K^+	Ca^{2+}	Mg^{2+}	Sr^{2+}	Fe^{2+}
1-4, 50-52	6.00	2.06	0.41	3.99	1.42	0.011	0.007
3-4, 125-127	16.25	1.77	0.35	3.74	1.36	0.012	0.009
4-3, 125-127	24.45	1.28	0.31	3.87	1.11	0.010	0.012
5-1, 125-127	31.15	1.00	0.20	4.37	0.95	0.011	0.008
5-5, 50-52	36.40	1.96	0.30	3.87	1.42	0.011	0.008
6-3, 125-129	43.85	NA[a]	NA	NA	NA	NA	NA
6-5, 125-129	46.85	0.63	0.13	3.62	0.72	0.007	0.005
7-3, 125-127	53.55	0.99	0.17	3.99	0.97	0.007	0.005
8-2, 125-127	61.75	0.89	0.17	3.74	0.88	0.006	0.016
9-2, 13-14	70.33	0.72	0.15	3.99	0.80	0.006	0.017
10-3, 94-95	82.34	0.60	0.11	3.87	0.74	0.006	0.012
12-1, 42-43	98.02	1.00	0.23	3.49	1.01	0.007	0.016
13-2, 42-43	109.12	1.07	0.25	3.99	0.97	0.008	0.009
15-1, 42-45	136.42	1.56	0.42	3.37	1.30	0.013	0.012
17-2, 58-60	147.78	1.35	0.36	3.74	1.15	0.013	0.008
17-3, 58-60	149.28	1.14	0.25	3.62	0.90	0.005	0.012

[a] NA = Sample not analyzed.

mostly carbonates and possibly small amounts of others such as sulfates, oxides, or sulfides, have developed since deposition, but only the amount of total carbonate in each sample was determined; the latter varies between 8.5 and 18.3%, and has an average of 13.6% for the samples analyzed.

Mineralogy of the clay fraction in Pigmy Basin sediments of Hole 619 was studied in detail, not only because of the abundance of clay minerals but also because they might yield signs indicative of incipient diagenesis. Mineralogical analysis of the clays show that, with two exceptions (Samples 619-6-3, 125–129 cm and 619-10-3, 94–95 cm) in which illite is abundant, smectite dominates the clay fraction of the samples. Averages for all samples are 48% smectite, 30% illite, and 23% total combined kaolinite–chlorite, with kaolinite being predominant over chlorite. These results agree well with those of a mineralogical study of clayey sediments in six gravity cores from the Gulf of Mexico by Scafe and Kunze (1971), and of shelf slope sediments off the coast of Texas–Louisiana by Hottman (1975). On the other hand, Zemmel and Cook (1972) report illite being the most abundant clay mineral in sediments of cores collected from near the top of Holes 91 and 92 drilled on DSDP Leg 10; the sediments in these cores are approximately equivalent in age and depth to those of this study. Hole 92 is located near the Sigsbee Scarp and Hole 91 is located in the Sigsbee Abyssal Plain. Devine et al. (1972), in a study of surficial sediments in the deep Gulf, also report the dominance of illite. Whether these discrepancies in the clay mineralogy result from differences in sediment source, degree of diagenesis, or simply different analytical techniques remains to be resolved.

Griffin (1962) characterizes clays carried by the Mississippi into the northwestern Gulf of Mexico as having 60–80% montmorillonite, 20–30% illite, and 10–20% kaolinite, with other clay minerals present in only minor to trace amounts. A comparison of Griffin's estimates with that of clay minerals found in the Pigmy Basin sediments reported here shows that the latter contain less montmorillonite (although it is still the most abundant) and proportionally more illite and kaolinite–chlorite. We believe that these changes are true and they result from postdepositional or diagenetic processes. This is further borne out by the general decrease of smectite and increase of the other clays with depth in Pigmy Basin.

Incipient diagenesis of clay minerals in the Pigmy Basin sediments is best illustrated by comparing the clay mineralogy data against bulk sample exchangeable cation data as shown in Figure 7. Data for exchangeable Ca^{2+} (Table 3) were not included in constructing Figure 7, because of the presence in the bulk sediment of cementing carbonates and other Ca^{2+}-bearing material. Figure 7 indicates the following: (1) the total ammonium acetate exchangeable K^+, Mg^{2+}, and Na^+ are unquestionably related directly to the amount of smectite in the clay fraction of the samples and (2) both smectite and exchangeable cations generally decrease with depth. This decrease is not systematic because there are differences between the samples other than clay mineralogy. For example, Samples 619-17-2, 58–60 cm and 619-17-3, 58–60 cm are from the chaotic zone in the lowermost part of the interval sampled and have probably undergone somewhat different burial history than the others. Also, Sample 619-10-3, 94–95 cm results are significantly different from the others, possibly because of the high amount of carbonate in that sample.

Depth-related changes in clay mineralogy and amounts of exchangeable cations in the Pigmy Basin sediments reflect primarily the effect of compaction with continued deposition. The principal conclusions of this study are (1) for the 150-m interval studied, the Pigmy Basin sediments had a constant source of supply and (2) incipient diagenesis, caused by mechanical compaction, has resulted in general decreases with depth in expandable clay minerals and exchangeable cations.

ACKNOWLEDGMENTS

This work was supported in part by the Center for Energy and Mineral Resources, Texas A&M University, Amoco Production Company, Tulsa, Oklahoma, and NSF Grant OCE-8315016. S. Ali and an anonymous reviewer reviewed an earlier draft of this manuscript.

REFERENCES

Alexiades, C. A., and Jackson, M. L., 1966. Quantitative clay mineralogical analysis of soils and sediments. *Clays Clay Miner.*, 14: 35–52.

Biscaye, P. E., 1965. Mineralogy and sedimentation of recent deep-sea clay in the Atlantic Ocean and adjacent areas and oceans. *Geol. Soc. Am. Bull.*, 76:803–832.

Bouma, A. H., 1983. Intraslope basins in northwest Gulf of Mexico: a key to ancient submarine canyons and fans. *Am. Assoc. Pet. Geol. Spec. Publ.*, 32:567–581.

Devine, S. G., Ferrell, R. E., and Billings, G. R., 1972. A quantitative x-ray diffraction technique applied to fine-grained sediments of the deep Gulf of Mexico. *J. Sediment. Petrol.*, 42:468–475.

Ericson, D. B., and Wollin, G., 1968. Pleistocene climates and chronology in deep-sea sediments. *Science*, 162:1227–1234.

Griffin, G. M., 1962. Regional clay-mineral facies—Products of weathering intensity and current distribution in the northeastern Gulf of Mexico. *Geol. Soc. Am. Bull.*, 73:737–768.

Hottman, W. E., 1975. Area distribution of clay minerals and their relationship to physical properties. Gulf of Mexico [M.S. thesis]. Texas A&M University, College Station.

Hutton, C. O., 1959. Mineralogy of beach sands between Half Moon and Monterey Bays, California. *Calif. Div. Mines Spec. Rept.*, No. 59.

Mehra, O. P., and Jackson, M. L., 1960. Iron oxide removal from soils and clays by a dithionite-citrate system buffered with sodium bicarbonate. *Clays Clay Miner.*, 7:317–327.

Scafe, D. W., and Kunze, G. W., 1971. A clay mineral investigation of six cores from the Gulf of Mexico. *Mar. Geol.*, 10:69–85.

Schultz, L. G., 1964. Quantitative interpretation of mineralogical composition from x-ray data and chemical data for the Pierre Shale. *U.S. Geol. Surv. Prof. Pap.*, 391-C:31.

Zemmel, I., and Cook, H. E., 1972. X-ray mineralogy studies of Leg 10 cores in the Gulf of Mexico. *In* Worzel, J. L. Bryant, W., et al., *Init. Repts. DSDP*, 10: Washington (U.S. Govt. Printing Office), 337–374.

Date of Initial Receipt: 29 March 1985
Date of Acceptance: 2 August 1985

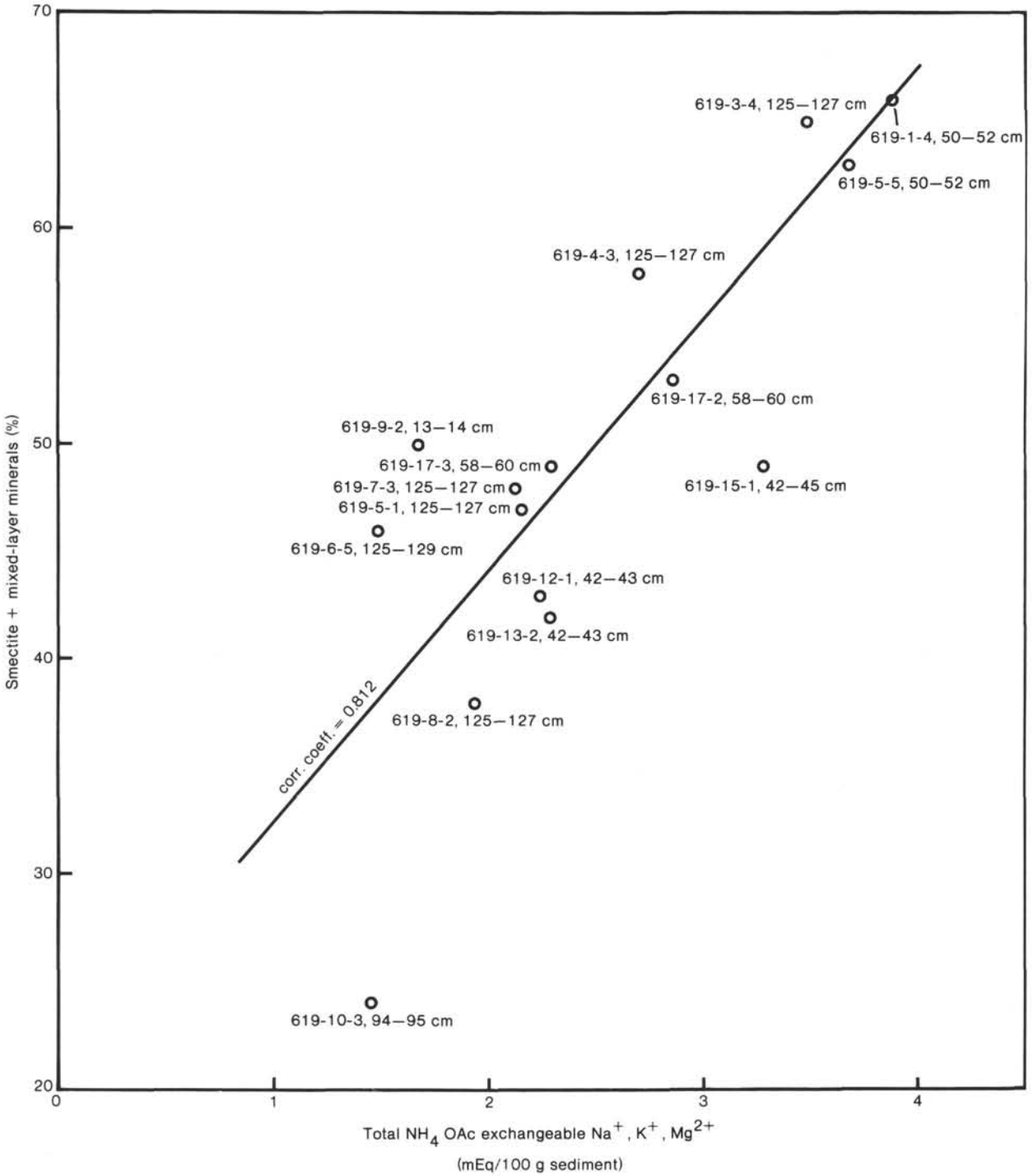

Figure 7. Plot of bulk sample ammonium acetate exchangeable Na^+, K^+, and Mg^{2+} versus percentage smectite + mixed-layer minerals in the clay fractions of samples from Hole 619. Note that the sample number is given alongside each point; there is a general trend of decrease in both smectite and exchangeable cations with depth, although a number of exceptions exist.